PAPER

NJC
www.rsc.org/njc

Complexes of hexamethylenetetramine with zinc-tetraarylporphyrins, and their assembly modes in crystals as clathrates and hydrogen-bonding network polymers†

Mikki Vinodu and Israel Goldberg*

School of Chemistry, Sackler Faculty of Exact Sciences, Tel Aviv University, 69978 Ramat Aviv, Tel Aviv, Israel. E-mail: goldberg@post.tau.ac.il

Received (in Durham, UK) 20th April 2004, Accepted 10th June 2004
First published as an Advance Article on the web 16th September 2004

This study reveals self-assembly patterns of the tetra(4-pyridyl), tetra(4-hydroxyphenyl) and tetra(4-carboxyphenyl) zinc porphyrin moieties when reacted with a hexamethylenetetramine ligand, forming 1 : 1 five-coordinate, 1 : 2 and 1 : 2 six-coordinate complexes, respectively. Detailed structural characterization of the supramolecular organization in the resulting ordered solids is reported. Crystals of the 1 : 1 complex (**1**) represent a common tetraarylporphyrin clathrate found earlier in the "porphyrin sponges". Those of the 1 : 2 complexes consist of multiporphyrin polymeric networks that are sustained by extensive hydrogen bonding, involving the four hydroxylic (in **2**) or carboxylic (in **3**) functional substituents as proton donors and the N-sites of the hexamethylenetetramine ligand as proton acceptors. The polymeric frameworks are characterized by three-dimensional (in **2**) or two-dimensional (in **3**) open architectures with wide interporphyrin voids; yet, they do not interpenetrate into one another, giving rise to the formation of open channels that perforate the corresponding crystals and are loosely occupied by guest species of the crystallization solvent. The pronounced effect of the hexamethylenetetramine ligand on the supramolecular aggregation is highlighted, by relating the current findings to previously designed networks of the porphyrin building blocks in question.

Introduction

We have studied recently, along with others, the self-assembly modes of the tetra(4-pyridyl)porphyrin (TPyP), tetra(4-hydroxyphenyl)porphyrin (TOHPP) and tetra(4-carboxyphenyl)porphyrin (TCPP) moieties, and of their metallated derivatives, in a comprehensive effort to design new ordered solids with potentially useful properties.[1–7] This has led to the discovery of a number of two-dimensional and single-framework three-dimensional supramolecular porphyrin based-networks sustained by direct interporphyrin hydrogen-bonding and coordination, or tessellated by external metal ion or organic ligand bridging auxiliaries. Noteworthy are the stable molecular sieve structures and zeolite analogs constructed from the ZnTPyP,[2] CoTCPP[6a] and ZnTCPP[7a] building blocks, and interweaved networks based on the ZnTOHPP units.[4] The use of symmetrically functionalized tetraphenylporphyrins of square-planar symmetry as supramolecular tectons in the formation of such network solids has deserved the most attention thus far.[8] Studies of porphyrin systems with reduced symmetry and a more versatile combination of the molecular recognition functions associated with them have been initiated as well,[9] in order to further diversify the intermolecular assembly tools that can be employed in the construction of multiporphyrin networks. In this report we demonstrate how the characteristic assembly modes of the ZnTPyP, ZnTOHPP and ZnTCPP building blocks can be modified by reaction of these species with hexamethylenetetramine (HTMA). HTMA is a strong tetradentate nucleophile, which readily coordinates to the zinc ion in the porphyrin core as an axial ligand (Scheme 1). It may act also as a strong proton acceptor in hydrogen bonds, in possible competition with the hydroxylic and carboxylic functions carried by two of the porphyrin units. It is important to note in this context that common O–H···O or O–H···N hydrogen bonds represent a relatively weak and thermodynamically labile interaction (with enthalpic contribution within 10–30 kJ mol^{-1} per such H-bond),[10] and only their cooperative expression in the assembly of supramolecular aggregates may carry adequate stabilization energy to yield structures with long-range order in two or three dimensions. Nevertheless, the directionality features make these interactions key elements in targeted solid-state synthesis.[11] Crystallographic characterization of the assembly patterns formed by the five-coordinate ZnTPyP–HTMA and six-coordinate ZnTOHPP–(HTMA)$_2$ and ZnTCPP–(HTMA)$_2$ complexes (their solvated crystals labeled as compounds **1**, **2** and **3**, respectively) throws light on the optimal supramolecular interaction of these pyramidal and bipyramidal units and utilization of their molecular recognition features. To the authors' knowledge crystal structures of metalloporphyrin complexes with HTMA as an axial ligand have not been reported as yet.

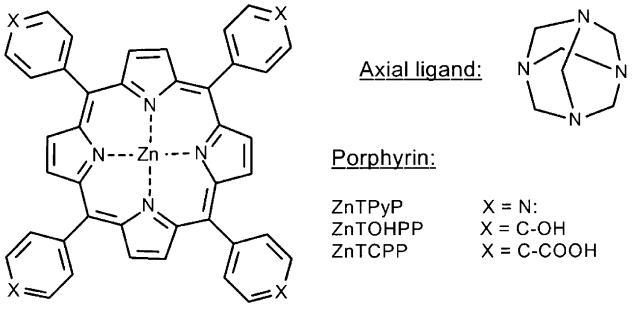

Scheme 1

† Electronic supplementary information (ESI) available: TGA–DTA diagrams for compounds **2** and **3**. See http://www.rsc.org/suppdata/nj/b4/b405945j/

DOI: 10.1039/b405945j

Experimental

The reagents and solvents were purchased from Mid Century [tetra(4-pyridyl), tetra(4-hydroxyphenyl) and tetra(4-carboxyphenyl) zinc(II)-porphyrin], Fluka (hexamethylenetetramine, nitrobenzene, ethylbenzoate), Merck (dimethylformamide) and Frutarom (chloroform and methanol). The porphyrin–HTMA complexes were obtained by reacting 1×10^{-5} mmol of the metalloporphyrin (6.83 mg of ZnTPyP, 7.43 mg of ZnTOHPP or 8.55 mg of ZnTCPP) with 4×10^{-5} mmol of HTMA in an appropriate solvent mixture (methanol–chloroform–nitrobenzene, methanol–nitrobenzene or DMF–ethyl benzoate, respectively). Single crystals suitable for X-ray diffraction were obtained by slow evaporation over several weeks. The identity of the obtained materials in a given reaction was confirmed in each case by repeated measurements of the unit-cell dimensions from different single crystallites. The inclusion-type crystals (see below) were found to be unstable in open air due to solvent escape associated with loss of good crystallinity, and their solvent content in parallel reaction batches was not always uniform. This prevented reliable characterization of the materials by combustion experiments. Their composition was thus determined by X-ray diffraction (**1**–**3**) and thermo-gravimetric (**2**, **3**) analyses.

The X-ray measurements (Nonius Kappa CCD diffractometer, MoKα radiation) were carried out at *ca.* 110 K, on crystals coated with a thin layer of amorphous hydrocarbon oil in order to minimize deterioration, possible structural disorder and related thermal motion effects, and to optimize the precision of the crystallographic results. The crystal and experimental data are summarized in Table 1. These structures were solved by direct methods (SIR-97) and refined by full-matrix least-squares on F^2 (SHELXL-97).[12] All non-hydrogen atoms were refined anisotropically. The hydrogens of the porphyrin and HTMA species were located in idealized positions, and were refined using a riding model with fixed thermal parameters [$U_{ij} = 1.2\ U_{ij}$ (eq.) for the atom to which they are bonded]. Those bound to the hydroxylic and carboxylic O-atoms and to water were located in difference-Fourier maps. Crystals of all three compounds contained a considerable amount of crystallization solvent, which in **2** and **3** could not be reliably modeled. Correspondingly, while the conventional refinement of **1** (including one molecule of water and half a molecule of nitrobenzene solvent) still converged to a reasonably low R_1 value of 0.059, those of **2** and **3** converged only at an R_1 value of 0.14 and 0.11 (while accounting for the porphyrin–HTMA complex only), respectively. In order to improve the refinement process of the main porphyrin fragment and the description of the interporphyrin assembly, the contribution of the disordered solvent in **2** and **3** was subtracted from the corresponding diffraction patterns by the Squeeze/Bypass procedure.[13] The calculated solvent-accessible volume was about 2328 Å^3 per unit-cell (36% of the unit-cell volume) in **2** and 599 Å^3 per unit-cell (34% of the unit-cell volume) in **3**,[13] allowing the inclusion of considerable amounts of solvent in the respective lattices. The actual solvent content in these crystals was assessed independently by thermo-gravimetric measurements, and amounts to ten molecules of nitrobenzene and two molecules of ethyl benzoate in the unit-cells of **2** and **3**, respectively. The TGA data suggest that in **2**, the nitrobenzene species are driven out of the crystal at around 109 °C, while the porphyrin host-compound decomposes near 215 °C. In **3**, molecules of the ethyl benzoate solvent escape the crystal upon heating within 120–220 °C, the ZnTCPP–$(HTMA)_2$ complex decomposes near 236 °C. Despite the solvent disorder, the crystallographic evaluations provided precise models of the porphyrin structure and intermolecular organization.†‡

Table 1 Crystal data and experimental parameters of the structural analysis

Compound[a]	**1**	**2**	**3**
Formula weight	901.81	1330.24	1434.85
Crystal system	Triclinic	Orthorhombic	Triclinic
Space group (no.)	$P\bar{1}$	*Pccn*	$P\bar{1}$
T/°C	−163	−163	−163
a/Å	9.1880(8)	18.7890(3)	10.3600(4)
b/Å	11.9360(6)	27.7420(5)	11.4980(6)
c/Å	20.4070(15)	12.4730(7)	15.3610(8)
α/deg	89.070(2)	90.0	76.002(2)
β/deg	79.492(3)	90.0	89.056(3)
γ/deg	71.746(6)	90.0	82.936(3)
V/Å^3	2087.7(3)	6501.5(4)	1761.8(2)
Z	2	4	1
μ(MoKα)/mm^{-1}	0.65	0.45	0.42
ρ_{calcd}/g cm^{-3}	1.435	1.359	1.352
$2\theta_{max}$/deg	50.0	55.7	56.4
Reflections collected	10 918	23 341	14 853
Unique reflections	6834	7467	8125
R_{int}	0.045	0.062	0.028
Reflections with $I > 2\sigma$	4910	4086	6025
R ($I > 2\sigma$)	0.059	0.055 (0.14)[b]	0.053 (0.11)[b]
R (all data)	0.090	0.094 (0.20)[b]	0.073 (0.13)[b]
R_w ($I > 2\sigma$)	0.140	0.147[b]	0.141[b]
R_w (all data)	0.157	0.159[b]	0.151[b]
$\lvert\Delta\rho\rvert_{max}$ e Å^{-3}	0.68	0.57[b]	0.65[b]

[a] Chemical formulae: **1**: $C_{40}H_{24}N_8Zn \cdot C_6H_{12}N_4 \cdot H_2O \cdot \frac{1}{2}(C_6H_5NO_2)$; **2**: $C_{44}H_{28}N_4O_4Zn \cdot 2(C_6H_{12}N_4) \cdot 2\frac{1}{2}(C_6H_5NO_2)$; **3**: $C_{48}H_{28}N_4O_8Zn \cdot 2(C_6H_{12}N_4) \cdot 2(C_9H_{10}O_2)$. [b] Based on diffraction data after the Squeeze/Bypass procedure (see text).[13] The data in parentheses refer to the original not "squeezed" intensities, excluding the disordered solvent which could not be modeled in the structure-factor calculations.

Results and discussion

The molecular structures of the metalloporphyrin complexes in **1**–**3** are shown in Fig. 1. In **2** and **3** units of the porphyrin complex are located on centers of crystallographic inversion. ZnTPyP and its analogs (with a different number of pyridyl functions or with metal ions other than zinc) are known to form chain coordination polymers in lipophilic solvents, and network coordination polymers in polar hydrophilic solvents, by ligation of the pyridyl function(s) of one porphyrin molecule to the metal ion core of adjacent unit(s).[1,2] However, HTMA is a much stronger nucleophile than a pyridyl function attached to porphyrin, and it can occupy more readily (also from entropy considerations by being smaller) the axial coordination site of the central zinc ion. The stereochemistry of divalent closed-shell d^{10} zinc in inorganic and organometallic compounds is characterized by high versatility, revealing coordination numbers from 2 to 8 and diverse geometries.[14] When inserted into the porphyrin core, the zinc ions commonly have coordination numbers 4 (square-planar), 5 (pyramidal) and 6 (octahedral), with 5 being especially common.[15] The latter is adopted in the reaction of ZnTPyP with HTMA. This five-coordinate compound of domed geometry (with the zinc ion deviating from the porphyrin plane towards the axial ligand) bears on its periphery only the N(sp^2) and N(sp^3) nucleophiles as functional groups, thus lacking an appropriate molecular recognition algorithm for interporphyrin self-assembly by specific interaction synthons other than dispersion. Not surprisingly, therefore, the ZnTPyP–HTMA aggregates in crystals as a true clathrate **1**, in a similar manner to that exhibited by many of the "porphyrin sponges" based on the zinc-tetraphenylporphyrin analog.[16]

‡ CCDC reference numbers 237489 (**1**), 237491 (**2**) and 237490 (**3**). See http://www.rsc.org/suppdata/nj/b4/b405945j/ for crystallographic data in .cif format.

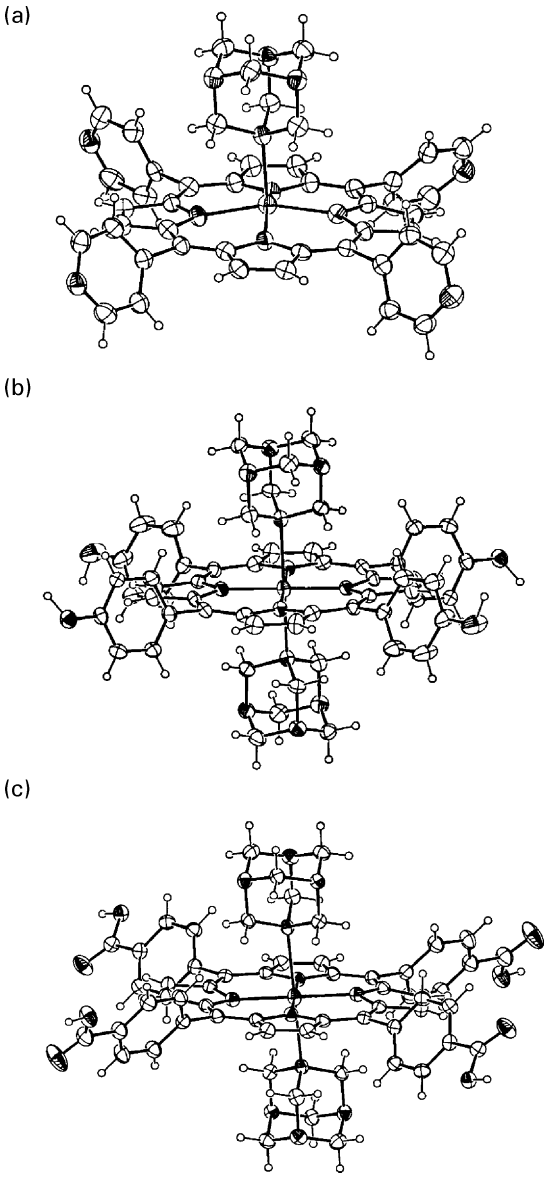

Fig. 1 The molecular structures of (a) **1**, (b) **2** and (c) **3** (the crystallization solvent is omitted). The thermal displacement parameters of the non-hydrogen atoms at *ca.* 110 K are represented by 50% probability thermal ellipsoids. The observed Zn–N(HTMA) coordination distances are: 2.189(3) Å in five-coordinate **1**, and 2.520(2) Å and 2.510(2) Å in six-coordinate **2** and **3**, respectively. The N, O and Zn atoms are represented by darkened ellipsoids.

The crystal structure of **1** consists of closely packed bilayers of inversion-related molecules (Fig. 2(a)), with the axial ligand of one species being positioned between the neighboring porphyrin units located above (or below) it. As commonly observed in the porphyrin clathrates, in areas of direct contact between adjacent porphyrin frameworks, typical π–π stacking and T-shaped pyridyl–pyridyl interactions can be observed. Side packing of adjacent layers is less complementary creating about 0.35–0.40 nm wide channel voids between the layers (Fig. 2(b)). These propagate through the crystal parallel to the *a*-axis, and accommodate the disordered molecules of nitrobenzene.

The most common mode of hydrogen-bonding-assisted assembly of ZnTOHPP observed earlier involves self-association of the porphyrin units through the *cis*-related hydroxyphenyl arms of neighboring moieties.[3] The basic motif that forms is a continuous one-dimensional polymer of interlinked coplanar porphyrin species. In some cases these linear porphyrin arrays are sufficiently close to one another to afford direct interporphyrin bridges between the chains as well, leading to the

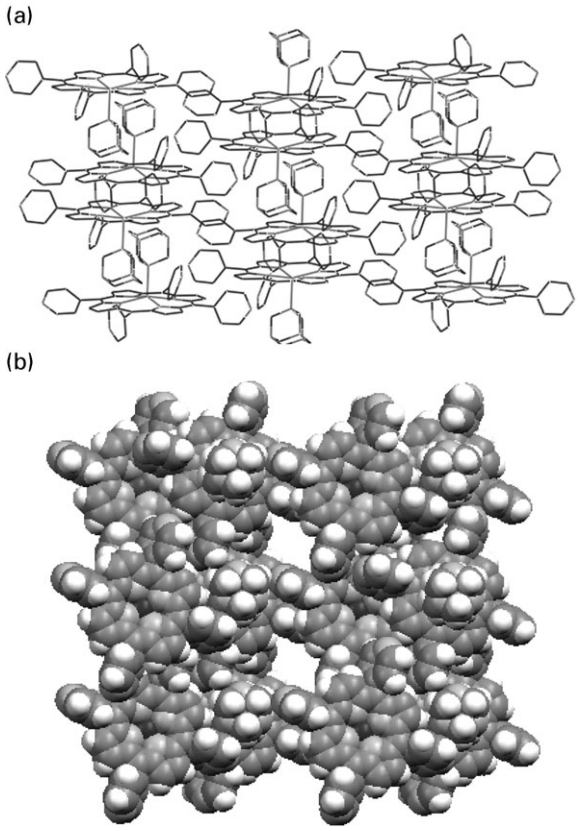

Fig. 2 Clathrate **1**. (a) The bilayered organization of the five-coordinate ZnTPyP–HTMA complexes (one layer is behind the other), showing the insertion of the axial ligand of one unit between the porphyrin frameworks of adjacent units. Note the domed conformation of the porphyrin core and the face-to-face alignment of pyridyl rings of adjacent species. (b) Space-filling illustration of the crystal structure viewed down the *a*-axis (*b* is vertical). It shows the contact zone between neighboring bilayers characterized by ∼0.4 nm wide channel voids that are occupied edge-on by the nitrobenzene solvent (not shown).

formation of layered two-dimensional aggregates. It has been further shown that reaction of ZnTOHPP with bipyridyl ligands leads to diverse modes of the intermolecular assembly due to the competing nature of the possible porphyrin–porphyrin OH···OH and porphyrin–ligand OH···N hydrogen bonds.[4] However, HTMA is characterized not only by a strong affinity to the zinc ions, but also by a remarkable tendency to act as a strong proton acceptor in hydrogen bonds, which is common to tertiary amines. Thus, the present reaction of ZnTOHPP with HTMA leads to a unique supramolecular assembly of these species, which is effected by optimization of the above features in a cooperative manner. Noteworthy is the preferred formation of the symmetric six-coordinate (rather than five-coordinate) ZnTOHPP–$(HTMA)_2$ complex in this case, as this increases the number of intermolecular hydrogen-bonds of the OH···N type and, correspondingly, their stabilizing contribution to the formed supramolecular assembly shown in Fig. 3. The supramolecular structure of **2** is sustained by extensive hydrogen bonding (Table 2). Every unit of the complex is involved in eight hydrogen bonds (using its four hydroxy groups as proton donors and four of the six available N_{HTMA}-sites as proton acceptors) to eight neighboring units of the porphyrin. The centers of the latter form a slightly distorted cube (Fig. 3(a)). Adjacent hydrogen-bonded molecules are related to each other by the screw/glide symmetry. Thus, given that the OH···N interaction is classified as a moderately strong hydrogen-bond with interaction energy of about 5 kcal mol^{-1} per bond,[10] the binding energy of the H-bonds associated with every building block amounts to ∼40 kcal mol^{-1}. Utilization of the coordination and hydrogen bonding potential of the

Table 2 Hydrogen-bonding parameters

O–H	N_{HTMA}	O–H/Å	H···N/Å	O···N/Å	O–H···N/°
Compound **2**[a]					
OH(1)	N(6) $(1-x, y+\frac{1}{2}, \frac{1}{2}-z)$	1.03	1.74	2.721(3)	158
OH(2)	N(4) $(x+\frac{1}{2}, -y, \frac{1}{2}-z)$	1.04	1.70	2.735(3)	180
Compound **3**[a]					
OH(1)	N(6) $(1-x, 1-y, 1-z)$	0.96	1.71	2.668(2)	174
OH(3)	N(5) $(x, y, z-1)$	0.84	1.86	2.691(2)	168

[a] Similarly N(6) at (x, y, z) interacts with OH(1) at $(1-x, y-\frac{1}{2}, \frac{1}{2}-z)$, and N(4) at (x, y, z) interacts with OH(2) at $(x-\frac{1}{2}, -y, \frac{1}{2}-z)$. [b] Similarly N(6) at (x, y, z) interacts with OH(1) at $(1-x, 1-y, 1-z)$, and N(5) at (x, y, z) interacts with OH(2) at $(x, y, z+1)$.

component species almost to capacity results in the formation of an open three-dimensional architecture of the hydrogen-bonded polymer. This networked arrangement of the ZnTOHPP–$(HTMA)_2$ entities is perforated by two sets of channel voids, which propagate through the crystal parallel to the *c*-axis (Fig. 3(b)). These channels are approximately 0.6 nm wide (van der Waals dimensions), and are accessible to other components from the crystallization environment. In **2**, they include severely disordered/diffused molecules of nitrobenzene.

The ZnTCPP building block is known to self-assemble into open two-dimensional flat arrays by hydrogen bonds, the specific interaction pattern of the self-complementary carboxylic functions of adjacent species [whether of the cyclic dimeric $(COOH)_2$, or chain polymeric $(\cdots CO_2H\cdots CO_2H\cdots CO_2H\cdots)$ type] depending to a large extent on the shape of the template applied in the networking process.[8] Networks in which every porphyrin unit is connected equatorially to four different porphyrins *via* the cyclic dimeric $(COOH)_2$ synthons (thus taking part in eight hydrogen bonds with its neighbors) are of a particular interest, as they contain a 1.6 nm wide interporphyrin void space. Such networks can either stack on top of each other in a nearly overlapping manner to yield a molecular sieve type material,[5a] or they can interweave into one another to self-fill the empty space.[5c] The preferred organization directed by the thermodynamically labile supramolecular synthons is highly dependent on the crystallization conditions.[5a] Then, the direct H-bonding interaction between the carboxylic sites can be intentionally disrupted by the use of either metal ions or strong proton acceptors inserted as bridging groups between neighboring carboxylic (or carboxylate) functions. Suitable examples in the former case are provided by microporous network architectures of the ZnTCPP tessellated by various metal cations and metal ion clusters,[7] some of them representing organic zeolite analogues.[6a,7a] In the latter context, it has been shown that the presence of strong proton acceptors such as dimethylsulfoxide can interfere with direct hydrogen bonding between the ZnTCPP species.[5b] A similar situation occurs in the present case, where the N-atoms of the HTMA ligand bound to the porphyrin core offer more attractive sites for hydrogen bonding than the carboxylic substituents of the TCPP framework. As in the previous example, the possibility of achieving a more extensive hydrogen bonding scheme induces the formation of six-coordinate ZnTCPP–$(HTMA)_2$ entities (rather than five-coordinate units as in **1**). The porphyrin fragment provides four proton-donating sites, while the two axial HTMA ligands provide the complementary proton acceptors (somewhat unexpectedly, the carboxylic groups are not active as proton acceptors in the present case). Structure **3** represents, however, a different hydrogen-bonding connectivity scheme to that observed in **2**. Here, every ZnTCPP–$(HTMA)_2$ building block associates only to four adjacent units related by either inversion or lattice translation, its linkage to each of the neighboring species involving two hydrogen bonds: $COOH\cdots N_{HTMA}$ and $N_{HTMA}\cdots HOOC$

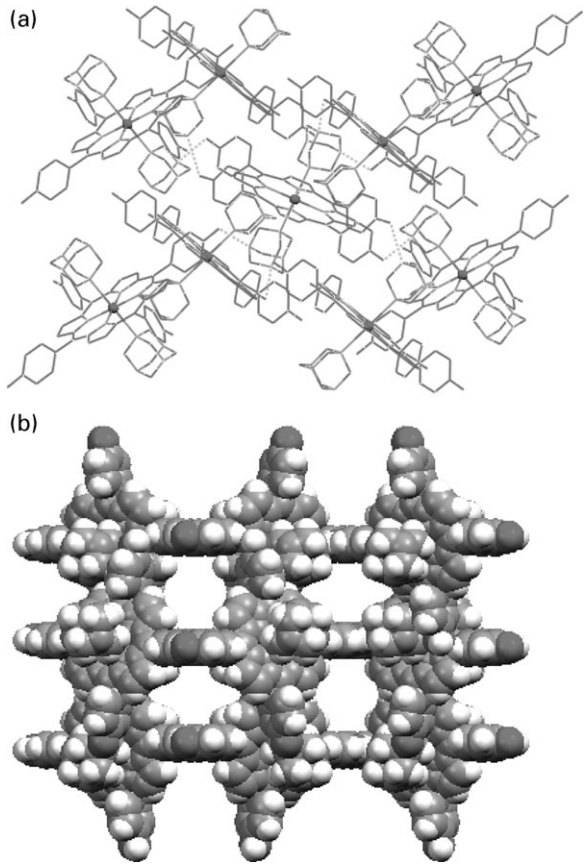

Fig. 3 Compound **2**. (a) Illustration of the hydrogen bonding between a given ZnTOHPP–$(HTMA)_2$ unit and eight surrounding moieties centered on vertices of a cubic polyhedron. Small spheres denote the metal ions. The hydrogen bonds are indicated by dotted lines. (b) View of the crystal structure down the *c*-axis (*b* is horizontal), showing the 0.6 nm wide channels that propagate through the crystal parallel to *c*, and are accessible to the crystallization solvent.

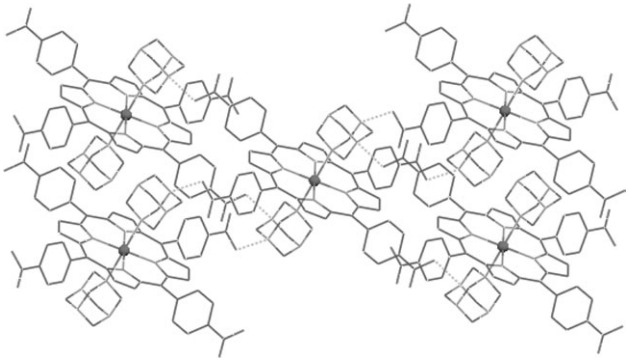

Fig. 4 Supramolecular hydrogen bonding scheme in **3**. Every ZnTCPP–$(HTMA)_2$ molecule is involved in four $COOH\cdots N_{HTMA}$ and four $N_{HTMA}\cdots HOOC$ interactions to four neighboring units related to the central one by either inversion or lattice translation. Small spheres denote the metal ions. The hydrogen bonds are indicated by dotted lines.

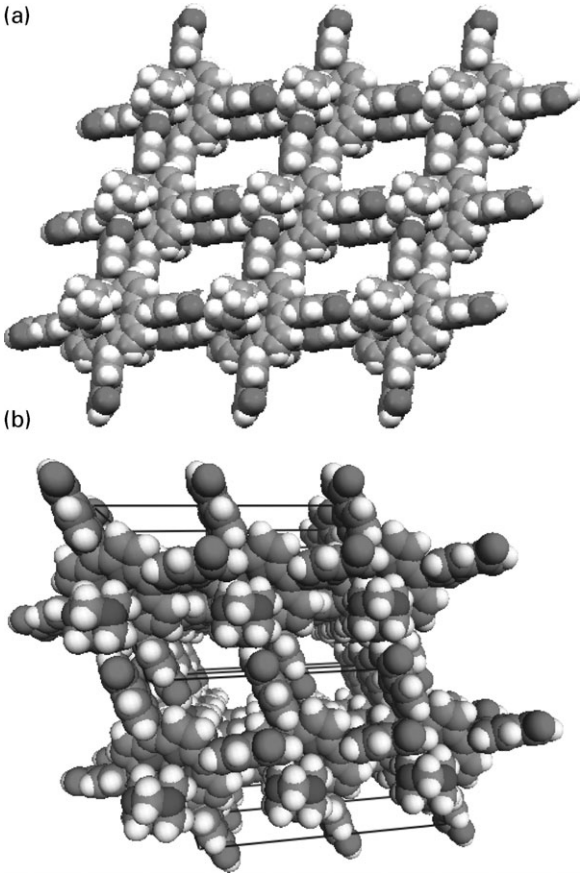

Fig. 5 (a) Space-filling illustration of the hydrogen-bonded corrugated layer of the ZnTCPP–$(HTMA)_2$ units in **3**, showing the paired interactions $COOH\cdots N_{HTMA}$ and $N_{HTMA}\cdots HOOC$ between two adjacent species along the four equatorial directions. (b) View of the crystal structure down the *a*-axis, along the open 0.5×0.8 nm^2 channels (crystallization solvent that occupies these channels in the crystal is omitted). Three H-bonded layers are shown edge-on.

(Fig. 4, Table 2). Extension of this binding pattern throughout the crystal yields corrugated two-dimensional layers, parallel to the (110) lattice plane, with large void space between adjacent units (Fig. 5(a)). In the crystal these layers are tightly stacked one on top of the other along the $a+b$ axis, with the convex surfaces of one layer (represented by the axial ligands) fitting into the concave areas (formed by the peripheral TCPP framework) of two adjacent layers from above and below. In the resulting arrangement wide channel voids of 0.5×0.8 nm^2 cross-section propagate through the crystal parallel to the *a*-axis of the unit-cell (Fig. 5(b)), to be filled by severely disordered ethyl benzoate crystallization solvent.

Conclusion

The above results demonstrate new types of porphyrin-based network materials (compounds **2** and **3**) supramolecularly organized into three-dimensional and two-dimensional open architectures by means of cooperative hydrogen bonding. They show that the use of strong nucleophiles and good proton acceptors can diversify the common aggregation modes of the functionalized metalloporphyrin building blocks, by offering alternative coordination and hydrogen bonding interaction synthons. The HTMA ligand proved very effective to this end due to its strong affinity for metal ions and proton acceptor function. The present work also revealed that enthalpic optimization of the intermolecular interactions affects the preferred porphyrin–HTMA coordination ratio (1 : 1 in **1** *vs.* 1 : 2 in **2** and **3**). It has been confirmed that a concerted utilization of the hydrogen-bonding attractions between large and rigid building blocks (following the rules described by Etter for organic crystals)[17] often has adequate driving force during the nucleation stage in solution for the preferred construction of 'microporous' supramolecular frameworks with long-range order that contain a large amount of open space.[18] The interporphyrin voids in **2** and **3** are smaller than the size of the individual building blocks, thus preventing network interpenetration. These findings provide further insight to our continuing crystal-engineering efforts of porphyrin based molecular sieve materials and zeolite analogues.

Acknowledgements

This research was supported in part by The Israel Science Foundation (grant no. 68/01).

References

1 E. B. Fleischer and A. M. Shachter, *Inorg. Chem.*, 1991, **30**, 3763–3769.
2 (*a*) H. Krupitsky, Z. Stein, I. Goldberg and C. E. Strouse, *J. Inclusion Phenom.*, 1994, **18**, 177–192; (*b*) K.-J. Lin, *Angew. Chem., Int. Ed.*, 1999, **38**, 2730–2732.
3 I. Goldberg, H. Krupitsky, Z. Stein, Y. Hsiou and C. E. Strouse, *Supramol. Chem.*, 1995, **4**, 203–221.
4 (*a*) Y. Diskin-Posner, G. K. Patra and I. Goldberg, *Chem. Commun.*, 2002, 1420–1421; (*b*) Y. Diskin-Posner, G. K. Patra and I. Goldberg, *CrystEngComm*, 2002, **4**, 296–301.
5 (*a*) Y. Diskin-Posner and I. Goldberg, *Chem. Commun.*, 1999, 1961–1962; (*b*) Y. Diskin-Posner, S. Dahal and I. Goldberg, *Chem. Commun.*, 2000, 585–586; (*c*) P. Dastidar, Z. Stein, I. Goldberg and C. E. Strouse, *Supramol. Chem.*, 1996, **7**, 257–270.
6 (*a*) M. E. Kosal, J.-H. Chou, S. R. Wilson and K. S. Suslick, *Nature Mater.*, 2002, **1**, 118–121; (*b*) D. Hagrman, P. J. Hagrman and J. Zubieta, *Angew. Chem., Int. Ed.*, 1999, **38**, 3165–3168; (*c*) C. V. K. Sharma, G. A. Broker, J. G. Huddleston, J. W. Baldwin, R. M. Metzger and R. D. Rogers, *J. Am. Chem. Soc.*, 1999, **121**, 1137–1144; (*d*) L. Carlucci, G. Ciani, D. M. Proserpio and F. Porta, *Angew. Chem., Int. Ed.*, 2003, **42**, 317–322.
7 (*a*) Y. Diskin-Posner, S. Dahal and I. Goldberg, *Angew. Chem., Int. Ed.*, 2000, **39**, 1288–1292; (*b*) Y. Diskin-Posner and I. Goldberg, *New J. Chem.*, 2001, **25**, 899–904; (*c*) Y. Diskin-Posner, G. K. Patra and I. Goldberg, *Eur. J. Inorg. Chem.*, 2001, 2515–2523; (*d*) M. Shmilovits, Y. Diskin-Posner, M. Vinodu and I. Goldberg, *Cryst. Growth Des.*, 2003, **3**, 855–863; (*e*) M. Shmilovits, M. Vinodu and I. Goldberg, *New J. Chem.*, 2004, **28**, 223–227.
8 (*a*) I. Goldberg, *CrystEngComm*, 2002, **4**, 109–116; (*b*) I. Goldberg, *Chem.–Eur. J.*, 2000, **6**, 3863–3870.
9 M. Vinodu and I. Goldberg, *CrystEngComm*, 2003, **5**, 204–207; M. Vinodu and I. Goldberg, *CrystEngComm*, 2003, **5**, 490–494.
10 G. A. Jeffrey, *An Introduction to Hydrogen Bonding*, Oxford University Press, Oxford, UK, 1997.
11 (*a*) G. R. Desiraju, *Angew. Chem., Int. Ed. Engl.*, 1995, **34**, 2311–2327; (*b*) F. Allen, P. R. Raithby, G. P. Shields and R. Taylor, *Chem. Commun.*, 1998, 1043–1044.
12 (*a*) A. Altomare, M. C. Burla, M. Camalli, M. Cascarano, C. Giacovazzo, A. Guagliardi and G. Polidori, SIR-97, *J. Appl. Crystallogr.*, 1994, **27**, 435–436; (*b*) G. M. Sheldrick, SHELXL-97, *Program for the Refinement of Crystal Structures from DiffractionData*, University of Göttingen, 1997.
13 (*a*) P. Van der Sluis and A. L. Spek, *Acta Crystallogr., Sect. A*, 1990, **46**, 194–201; (*b*) A. L. Spek, *Acta Crystallogr., Sect. A*, 1990, **46**, C34.
14 See for example: F. A. Cotton and G. Wilkinson, in *Advanced Inorganic Chemistry*, Wiley & Sons, New York, 1980.
15 See in Cambridge Structural Database: F. H. Allen, *Acta Crystallogr., Sect. B*, 2002, **58**, 380–388.
16 (*a*) M. P. Byrn, C. J. Curtis, Y. Hsiou, S. I. Khan, P. A. Sawin, S. K. Tendick, A. Terzis and C. E. Strouse, *J. Am. Chem. Soc*, 1993, **115**, 9480–9497 and references therein; (*b*) R. Krishna Kumar, S. Balasubramanian and I. Goldberg, *Inorg. Chem.*, 1998, **37**, 541–552.
17 M. C. Etter, *J. Phys. Chem.*, 1991, **95**, 4601–4610.
18 (*a*) P. Brunet, M. Simard and J. D. Wuest, *J. Am. Chem. Soc.*, 1999, **119**, 2737–2738; (*b*) M. J. Zaworotko, *Nature*, 1997, **386**, 220–221; (*c*) H. J. Choi, T. S. Lee and M. P. Suh, *Angew. Chem., Int. Ed.*, 1999, **38**, 1405–1408.